NAZARBAYEV UNIVERSITY

CHARACTERIZING THE BIOPHYSICAL PROPERTIES OF NORMAL AND CANCER NEURAL STEM CELLS

Dana Kulseiit
(B.Sc., al-Farabi Kazakh National University)

A THESIS SUBMITTED
FOR THE DEGREE OF MASTER OF SCIENCE IN BIOLOGICAL SCIENCES
DEPARTMENT OF BIOLOGY SCHOOL OF SCIENCES AND HUMANITIES
NAZARBAYEV UNIVERSITY
2022

Student: Dana Kulseiit  24.06.2022

Supervisor: Dr. Tri Pham  24.06.2022

DECLARATION

I hereby declare that the thesis is my original work and it has been written by me in its entirety. I have duly acknowledged all the sources of information which have been used in the thesis. This thesis has also not been submitted for any degree in any university previously.

Dana Kulseiit

24 June 2022

ACKNOWLEDGEMENTS

All work shown in this thesis project was performed under the direct supervision of Dr. Tri Thanh Pham. I want to express my gratefulness to Dr. Pham for opening me the world of mechanobiology, for his guidance as well as experience and knowledge shared. I learnt to aim carrying out only high standard and thorough work from him for which I am very happy and thankful.

I want to express my gratitude to all former and current Mechanobiology laboratory members at Nazarbayev University for great memories and useful discussions. It is a pleasure to thank my group- and lab-mate Timur Elebessov for supportive talks and for teaching me all the procedures required for the cell size measurements. Thanks to Meruyert Tilegen's assistance in drawing the boundaries of cells on Fiji, I was able to measure the cell cross-sectional area on time. Moreover, I want to thank her for emotional support and help with AFM experiments. I am extremely grateful for my colleague Faisal Nazir, who trained me on atomic force microscopy and helped me with AFM tips and experiments. Furthermore, Faisal provided a lot of emotional support and taught me how to make AFM data processing. I also thank Ayazhan Dauletova for her feedback on proofreading this thesis and for good memories.

I am thankful to my friends for having funny memories about these two years during our Master's program.

Further I want to express my gratitude to my family for believing in me and supporting me.

TABLE OF CONTENTS

ABSTRACT

Cancer is one of the leading causes of deaths worldwide accounting for 10 million people deceases in 2020. Metastatic spreading is the key feature that makes cancer difficult to cure. Stiffness and adhesion of cancer cells were found to be altered during metastasis, leading to a hypothesis that these changes are correlated with their migrating ability. In this project, we explore whether there is a difference between normal and cancer cells based on their biophysical and biomechanical properties such as cell cycle and mitosis times, cell cross-sectional area, spindle length, and cortical stiffness. *Drosophila melanogaster* neuroblasts (NBs) were used as a model for this study. The results revealed that *pins* mutant and *brat* mutant NBs mitosis times are similar to wildtype in S2 medium, however *pins* mutant NBs have longer mitosis times in comparison to wildtype and *brat* mutant NBs in CGS. With regard to cell cycle times in S2 medium, there is no significant difference between wildtype and *brat* mutant neuroblasts. Additionally, *pins* mutant NBs turned out to be softer and smaller in size compared to wildtype and *brat* mutant NBs. Therefore, we concluded that depending on the type of cancer or mutation, the cells may display different biophysical and biomechanical properties in contrast to their wildtype counterpart.

Keywords: *Drosophila* neuroblast, live cell imaging, atomic force microscopy.

LIST OF TABLES

LIST OF FIGURES AND ILLUSTRATIONS

ABBREVIATIONS

NB	Neuroblast
GMC	Ganglion Mother Cell
INP	Intermediate Neural Progenitor
Brat	Brain tumor
Pins	Partner of Inscuteable
CGS	Chan & Gehring solution
S2	Schneider insect medium
NEB	Nuclear Envelope Breakdown
AO	Anaphase Onset
CC	Complete Cytokinesis
AFM	Atomic Force Microscopy

1 INTRODUCTION

1.1 Cancer

1.1.1 Cancer causes, diagnostics, treatment

A tumor is an abnormal mass of cells which is accumulated because of uncontrolled cell proliferation. It can be either benign or malignant. Benign tumor is characterized by slow growth, presence of distinct borders and absence of invading potential to surrounding tissues and organs, whereas all opposite characteristics are true for malignant tumor (https://www.who.int/news-room/fact-sheets/detail/cancer).

According to World Health Organization (WHO), cancer (malignant tumor or neoplasm) is a large group of diseases that can get initiated in almost any part of the body. This process is associated with chaotic growth of abnormal cells with the potential to invade or spread to other tissues or organs, forming a secondary tumor. This cancer distribution throughout organs is known as metastasis which is the major cause of death.

Cancer is one of the leading mortal diseases around the world accounting for almost 10 million deaths in 2020. According to statistics, nearly half of the people diagnosed with cancer die each year. For example, if 9.6 million people out of 18.1 million died in 2018 worldwide, the similar tendency took a place in Kazakhstan, where about 14000 people out of approximately 32000 passed away (https://onco.kz/o-rake/ponimanie-raka/statistika-raka/). The most lethal cancer type is lung cancer that killed 1.8 million people worldwide in 2018 (https://www.who.int/news-room/fact-sheets/detail/cancer). On the other hand, breast cancer is the most frequently found malignant tumor both worldwide and in Kazakhstan.

What is the cause of cancer? The neoplasm formation possibility grows dramatically with age. This is mostly because of combination of factors like improper cell division arising with aging and cellular repair mechanisms inefficiency as well as built-up chronic diseases. Aside age, there are many other factors that play a crucial role in cancer formation. According to the International Agency for Research on Cancer (IARC), sunlight, tobacco, pharmaceuticals, alcohol, parasites, fungi, bacteria and some others are found to be carcinogens (https://www.who.int/news-room/fact-sheets/detail/cancer). They can be classified based on their nature as following:

- Biological carcinogens: infections from parasites, viruses (HIV, hepatitis B virus, hepatitis C virus, HPV, Epstein-Barr virus) and bacteria (*Helicobacter pylori*) (Blackadar, 2016);
- Chemical carcinogens: tobacco, asbestos, aflatoxin (a food contaminant), and arsenic (a drinking water contaminant);
- Physical carcinogens: ultraviolet from sunlight or artificial tanning devices and ionizing radiation.

Additionally, there is a basic set of risk factors which can enhance the malignant tumor formation. These are: unhealthy diet, alcohol consumption, rare or no physical activities, air pollution and others. In 2018, roughly one in ten people diagnosed with cancer gained the tumor due to carcinogenic infections, according to WHO.

Basically, there is a higher chance of survival for cancer patients if the tumor is identified at its early stage, followed by effective treatment. This is especially true for frequently found cancer types: breast, cervical, colorectal cancers that have high cure rates at initial stages and under appropriate treatment. The strategies as early diagnosis and screening were developed for increasing the survival rate of cancer patients. However, not all people

are aware of cancer initial symptoms, though early diagnosis is based on the patient knowledge and actions like seeking the medical advice. Screening, on the other hand, is about determining pre-cancer stage patients that have no symptoms developed yet. This program demonstrated its high efficiency for some but not all cancer forms. For instance, cervical cancer screening known as pap test does indeed save lives. According to statistics, 92% of cervical cancer cases found after this screening method, can be totally cured, while this percentage drops to 66% for cancer cases revealed due to symptoms (Denise Mann, 2012). However, screening is a complex process that requires a lot of resources like special equipment and well-trained staff.

Detection of cancer is followed by treatment option choice that involves surgical removal of the tumor, chemo- and radio-therapy that can be applied alone or in combination. Obviously, the decision is made by experts based on the tumor type, its stage and other factors. However, the metastatic spreading feature of cancer heavily impacts on the ability to fully treat the tumor. Therefore, up to date, the world is facing the problems of late-stage detection, expensive or unavailable diagnostics as well as inefficient therapy that are consequently retarding the cancer fighting ability.

1.1.2 Biophysical properties of normal and cancer cells

Many discoveries about cancer and its properties were made in the last twenty years using different approaches in various fields including biophysics. From breast palpation practices both in medicine for human and in studies on whole mouse mammary glands it is known that breast tumors are noticeably stiffer than the neighboring tissues which is explained by relative stiffening of the peripheral tumor stroma (Butcher *et al*, 2009; Schwartz *et al*, 2000). A supporting observation showed that during cancer progression

there is a rise in matrix deposition and in number of crosslinking in 3D cell cultures as well as in mouse mammary glands (Plodinec *et al*, 2012).

Paradoxically, it is estimated that single cancer cell cultures are softer than their healthy cell analogues (Diganta Dutta *et al*, 2020). However, they can change their stiffness- a measure of the cell surface resistance to an applied external force - when in contact with certain microenvironments due to their mechano-sensitivity (Abidine *et al*, 2018; Pham *et al*, 2019). For instance, cancer cells can regulate their cytoskeleton in a way that the cell is able to adhere to a specific surface. This mechanism can be applied when cancer cells invade to neighboring tissues or organs in order to deform to appropriate sizes and shapes (Suresh, 2007). The evidencing study of Cross et al. discovered that metastatic cells found in pleural fluid, which is a build-up excess fluid found outside lungs, were softer than normal cells, meaning that the lower stiffness positively affects the migration ability of cancer cells (Cross *et al*, 2007). Nowadays more and more researches are proving that abnormal proliferation and spreading of cancer is a result of mechanical feature changes in cancer cells. For example, cancer cell adhesion, migration and polarity are affected during metastasis (Wullkopf *et al*, 2018; Yadav *et al*, 2019; Nagelkerke *et al*, 2015).

Since metastasis is considered as the leading cause of cancer mortality, majority of efforts are directed to study more about this process. In one of such researches Mohanty et al. organized experimental metastasis assay, where they have intravenously injected human cancer cells into the immunocompromised mice via their tail. After a while mice were dissected and the cancerous tissues were observed under the stereoscopes, meaning that the human cancer cells could spread to the body of the mice. The resulting metastatic cells were isolated, cultured *in vitro* and injected to other healthy mice. When they have

compared the metastatic potential of latter cells with parental line, it was shown that spreading ability was enhanced in cells derived from metastases (Mohanty & Xu, 2010). Some recent discoveries were made in the last two years about the biophysical properties' changes in cancer cells. During metastatic spreading, the cancer cells travel from one organ to another via blood vessels that dictate a restricted cell shape in order to fit and be transported. These external forces may alter the cancer cell shape as well as may lead to permanent changes in internal organelles of the cells (Young *et al*, 2021; Follain *et al*, 2020). The cell nucleus was found to become softer under the mechanical stress which was correlated with a DNA protection. The softening of the nucleus was shown to be the result of heterochromatin deprivation (Nava *et al*, 2020). Another study employed the atomic force microscopy (AFM) to compare the stiffness of cancer cells and normal cells under hyperglycemic stress. In normal conditions, benign mammary epithelial cells were stiffer than breast cancer cells. In contrast, both cancer and normal cells became softer in response to increased concentrations of glucose, where cancer cells, in particular, were affected so much, that they have completely lost their elasticity (Diganta Dutta *et al*, 2020). The softening of cancer cells more than healthy cells creates a correlation between the cell's low stiffness and cancer progression. These finding suggest that decreasing the glucose consumption in patients with cancer (liver, colon and breast cancer) could improve their situation. Moreover, several researches showed that the biophysical properties of internal tissues impact the cancer cells behavior, including chemosensitivity and basic cell processes as cell growth, proliferation, migration and so on (Sarwar *et al*, 2020; Chaudhuri *et al*, 2020). Furthermore, there was an interesting finding in nuclear and cytoskeletal stiffness of normal and cancer cells. Fischer et al. showed that the nuclear stiffness of breast cancer cells as MDA-MB-231 and MCF-7 is higher than cortical

stiffness, whereas the opposing results were true for healthy mammary epithelial cells (Fischer *et al*, 2020).

Although there was a plenty of attempts to study and discover cancer cell properties and their behavior, none of them were dedicated to systematically characterize and compare the biophysical and biomechanical properties of normal and cancer cells that were sharing the same lineage. Moreover, up to date there is no information about the effect of cell intrinsic biophysical property like cell stiffness on cell physical and biological behavior, though this is a big question of interest in cell biology.

1.2. *Drosophila melanogaster*

Drosophila neuroblasts or neural stem cells are the precursors of the fly's central nervous system. The neuroblasts provide an appropriate model to explore the biophysical properties of normal and cancer cells based on the bond between asymmetric cell division and tumorigenesis. It was found that mutations in *brat* (transcriptional repressor, brain tumor), *lgl*, *dlg* and related genes lead to brain tumor in *Drosophila.* The neural stem cells of these mutants cannot give rise to differentiated cells, thus increasing the number of neuroblasts in the brain and leading to over-propagation as in tumors. When transplanted to adult fly abdomen these brain cells behave as cancer cells forming metastases and altering the original number of chromosomes (Knoblich, 2010; Woodhouse & Chuaqui, 1997). Additionally, the similar transplantation assay carried out on *pins* mutant (Partner of Inscuteable) neuroblasts revealed that they also cause metastatic cancer in the host fly (Caussinus & Gonzalez, 2005).

1.2.1 Applications of *Drosophila* in life science research

Drosophila melanogaster trivially known as fruit fly is a model organism that has been used in biological and genetic researches for over a century. Nowadays many areas of

modern medicine are built on the foundations laid by the studies on *Drosophila* about hereditary role of chromosomes, mutation generation via irradiation, early embryo development control and so on (Tolwinski Nicholas, 2017). Different breakthrough in various fields of biology including genetics, developmental biology, physiology, nervous system, stem cell biology, behavioral sciences were made by studying these flies.

The benefits of using fruit flies as a research model are:

- Easy and cheap to maintain
- Fast generation (~10 days) and short life span (2 months)
- Large number of progenies
- No ethical considerations
- 75% similarity with human (Reiter *et al*, 2001)
- Genetics is simple and easy to manipulate
- Well-studied anatomy
- Ease of dissection and visualization of complex tissues

Moreover, today's techniques applied for *Drosophila* studies enable to specifically alter the gene expression of a certain cell type with single cell precision *in vivo* in any organs and tissues including the nervous system. These genetic tools allow to find new roles of existing genes in the net of genetic interactions. In terms of fly genome, it is fully sequenced, a lot of loss-of-function mutants for high number of genes are created and are available, genes can be manipulated in numerous ways including targeted mutagenesis knock-outs, insertional mutagenesis and RNAi, overexpression can be achieved with spatial and temporal precision. Additionally, cell-type specific reagents are available to carry out the phenotypic and genetic analyses *in vivo* in CNS, for example. (Bellen *et al*, 2004; Brand & Perrimon, 1993)

Though *Drosophila melanogaster* is not the only model organism used in biology, flies are not losing their importance due to their high efficiency and new technologies that keep using them to discover more about fundamentals of life. Therefore, *Drosophila* flies are currently continuing to be used as "test tubes" for discovering genetic basis of disease related mechanisms, like of cancer, metabolic disorders, neurodegenerative disorders and so on (Tolwinski Nicholas, 2017).

1.2.2 *Drosophila* neuroblasts as a model for studying cancer

Neuroblasts (NBs) are fundamental for neurogenesis or the development of the nervous system, being the precursor cells of neurons (Knoblich, 2010). Neuroblasts are subdivided into type I, type II and type 0 (Figures 1, 2), they are different in terms of daughter cells produced. All NBs divide asymmetrically giving rise to one self-renewed neuroblast and one ganglion mother cell (GMC) in case of type I NB; or intermediate neural progenitor (INP) in case of type II NB; or a post-mitotic differentiating neuron in embryonic type 0 neuroblasts (Harding & White, 2018).

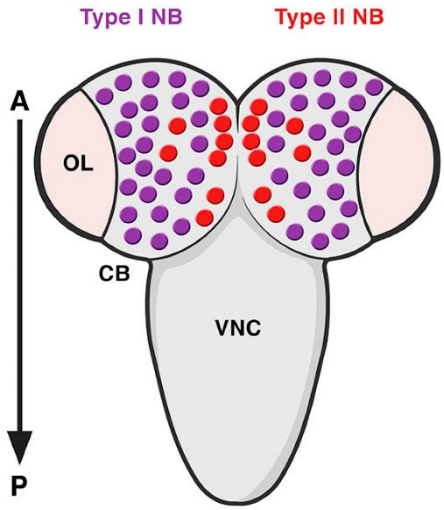

Figure 1. *Drosophila* larval brain morphology. The brain consists of two lobes indicated as CB (central brain) and ventral nerve cord (VNC). Each brain lobe has type I (purple) and type II (red) NBs. OL- optic lobe, A- anterior, P- posterior. (Carmena, 2020)

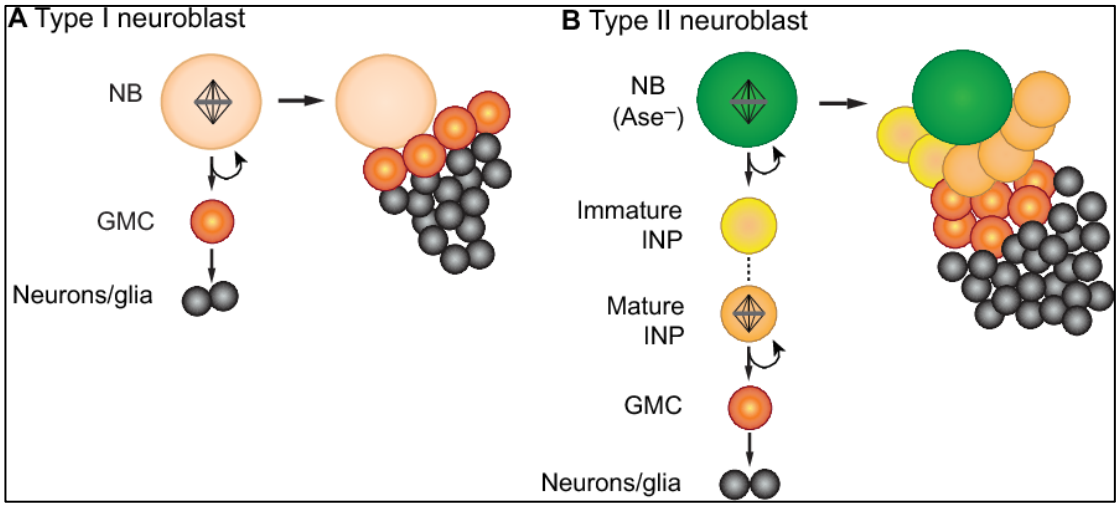

Figure 2. Type I and type II neuroblasts and their mode of division. (A) Type I NB divides asymmetrically to produce one GMC (orange) and one self-renewed NB. GMC divides further to produce neurons or glia (grey). (B) Type II NB divides asymmetrically to self-renew and to generate immature INP (yellow). Immature INP can divide symmetrically, to increase the pool of INPs. After maturation, INPs (peach color) divide asymmetrically to produce GMC and a self-renewed mature INP. GMC then divide once to produce differentiated neurons or glia. (Homem & Knoblich, 2012)

Resulting daughter cells of NBs are asymmetric in terms of size: neuroblast (10.9 ± 1.0 μm) is bigger than GMC (4.4 ± 0.6 μm) (Fuse *et al*, 2003) and in terms of fate, since neuroblast type I keeps dividing in the same manner up to 100 times, thus generating about 100 GMCs, while GMCs do not self-renew and differentiate into neurons or glial cells (Roubinet & Cabernard, 2014; Sanes *et al*, 2012; Pham *et al*, 2019). In the case of neuroblast type II division, immature INP is formed, which divides symmetrically to produce more INPs. When the sufficient amount is produced, they mature and divide asymmetrically to produce GMC and one self-renewed INP. As a result, type II neuroblasts can generate more GMC and neurons or glial cells via multiplication of these intermediate neural progenitors, than type I neuroblasts. This is compensated by amount of these two types of neuroblasts per brain lobe, being 80 for type I neuroblasts and 8 for type II neuroblasts (Weng & Cohen, 2015).

Another intrinsic feature of neuroblasts is their polarity (Homem & Knoblich, 2012; Gallaud *et al*, 2017). This property is regulated during cell cycle, thus playing a crucial role in spindle geometry and a correct asymmetry of daughter cells. (Cabernard & Doe, 2009). For a proper asymmetric cell division neuroblasts require two sets of proteins to be separately localized on the apical and basal cortex (Figure 3). For example, proteins like Numb (The Notch inhibitor), Prospero (transcription factor), Brat, Pon (partner of Numb), Staufen and Miranda are located asymmetrically on the basal side of the cell during mitosis. Consequently, these proteins are inherited by newly formed GMC to set its proper cell fate (Fuse *et al*, 2003).

On the other hand, apical cortical crescent has its own set of proteins consisting of Par complex (Bazooka, Par6 and aPKC) that recruits Inscuteable, which in turn enrolls Pins, Mud and Gαi. These proteins are important for the regulation of mitotic spindle orientation according to apical-basal axis. Moreover, they direct the cell fate determinants (Numb, Pros, Brat, etc) to be localized on the basal cortex. In contrast to cell fate determinants, apically localized proteins get degraded during anaphase (Knoblich, 2010).

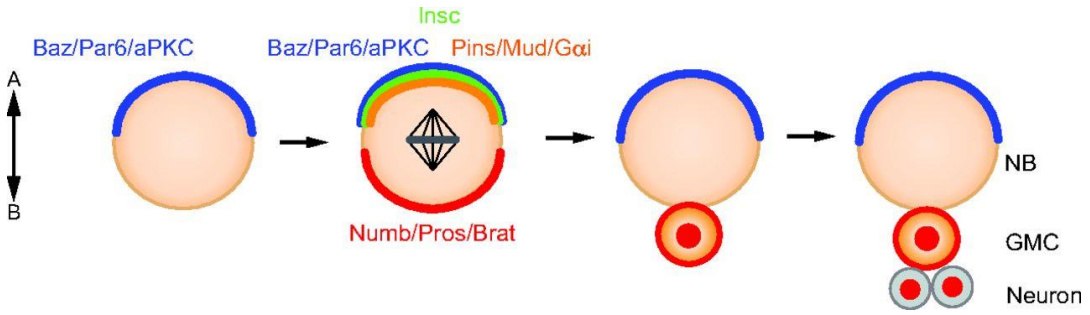

Figure 3. Asymmetric cell division in *Drosophila* neuroblasts. Baz/Par6/aPKC, Insc, Pins/Mud/Gαi are apically localized proteins, while Numb/Pros/Brat proteins are basally localized cell fate determinants. Basal proteins are inherited by GMC (Knoblich, 2010).

Four steps of neuroblast division can be identified in terms of polarity: establishment of polarity axis; mitotic spindle correct positioning; biased localization of cell fate determinant proteins on the basal cortex; as well as asymmetric segregation of these

proteins among two daughter cells. Interestingly, NBs inherit these apical-basal polarity cues from their "ancestors"- epithelial cells in the neuroectoderm, from which NBs delaminate. As mentioned, NBs have Par complex, an apically localized complex of proteins. It is believed that the neuroblast centrosome plays a role of a reference point attracting the Par complex to be apically localized during interphase. This in turn sets up an apical-basal axis of polarity within a neuroblast (step 1) (Rebollo *et al*, 2009). Afterwards, the spindle orientation is connected to the established apical basal polarity via Bazooka protein, a member of Par complex. Mud protein, which is a member of Pins complex, binds to the astral microtubules and thus is able to guide the spindle orientation (step 2). The next step is biased localization of cell fate determinant proteins on the basal cortex. This is maintained by aPKC (atypical protein kinase C) phosphorylation of Numb protein. During mitosis onset the protein called Aurora A kinase phosphorylates the protein Par-6, which subsequently leads to phosphorylation of another protein named Lgl. It reduces the bonds between Lgl and Par-6 and aPKC, therefore Par-3 protein replaces Lgl in this complex. When the new complex is formed, aPKC is able to phosphorylate the Numb protein on apical membrane of the cell, thus not allowing Numb protein to bind to the apical side of the cell via its phospholipid interactions. As a result, Numb complex is always localized basally in healthy neuroblasts (step 3) (Knoblich, 2010). It is followed by the last step- asymmetric segregation of cell fate determinants in favor to GMC which is led by other adaptor proteins called Miranda and Pon. During mitosis Miranda protein inhibits the transcription regulation of the neuroblast by a protein Prospero by linking it to the basal cortex of NB. Brat proteins is also linked to the basal cortex via Miranda, thus all of three proteins are segregated into the GMC. As soon as GMC is formed, Miranda protein is degraded, thus allowing cell fate determinants to do their job. For example,

Prospero enters the nucleus in order to foster the differentiation. Partner-of-Numb aids the biased localization of Numb as well as its biased segregation into GMC. (Knoblich, 2010).

The cell size asymmetry is additionally controlled by unequal distribution of non-muscle myosin II, as a result of which self-renewed neuroblast is always bigger than GMC. During anaphase, the neuroblast undergoes a cortical extension which is highly asymmetric, where the apical cortex expands 3 times more than the basal cortex. In regards to myosin II, both in symmetrically and asymmetrically dividing cells it is distributed uniformly around the cell cortex during prophase. When the cell enters anaphase, in symmetrically dividing cells the myosin II is saturated in the cell's equatorial region. However, in the case of neuroblast's anaphase, non-muscle myosin II is hold in the basal cortex of the cell together with Pavarotti and Anillin (furrow proteins). As a consequence, an apical depletion of non-muscle myosin II is generated that allows the apical expansion during anaphase, whereas the basal extension is restricted (Connell *et al*, 2011).

1.2.2.1 *Brat* mutant neuroblasts

There are 3 crucial components of basal domain proteins or cell fate determinants: Numb, Prospero, and Brat (Betschinger *et al*, 2006; Knoblich *et al*; Joe Hirata *et al*, 1988). Brat protein is asymmetrically segregated to the intermediate progenitor or GMC and it is important for the inhibition of cell self-renewal and for fostering the further differentiation into neuron and/or glial cell (Betschinger et al, 2006; Lee et al, 2006). The mutation in any of these genes disrupts the neuronal tissue balance resulting in an excess of NBs in larval brains. Although the mechanisms of *Numb* and *Prospero* work are well

studied, the specific function of *Brat* in neuroblasts is not clear (Choksi *et al*, 2006; Couturier *et al*, 2013).

As mentioned, there are different types of neuroblasts: type 0, type I, type II. All types of NBs express *Deadpan* (*Dpn*), which is a transcriptional repressor (Lee *et al*, 2006b). When the immature INP is formed from type II NB, it switches off the *Dpn* expression and activates the *Asense* (*Ase*) transcription factor, thus allowing for a symmetric division of INP. When the sufficient amount of immature INPs are formed, *Dpn* expression is activated, thus promoting asymmetric division of matured INPs (Boone & Doe; Bello *et al*, 2008).

In case of *brat* mutant type II neuroblasts, produced immature INPs cannot reinitiate the expression of *Dpn* and *Ase*. Consequently, these cells enter a temporary cell cycle block and eventually turn back to type II NBs. In the end, there are self-renewed NBs and the cells dedifferentiated into NBs, that in complex create an excess in pool of neuroblasts inside the brain, thus giving rise to transplantable brain tumor (Bowman *et al*, 2008).

Brat is a neoplastic tumor suppressor gene, meaning that when it is mutated, neoplastic tumors are formed or organs are overgrown and the cells arrangement is abnormal (Arama *et al*, 2000). In wildtype larvae Brat protein plays role in down regulating the ribosomal RNA synthesis. However, when its gene is mutated, the cell growth is enhanced as well as number of rRNA in nucleoli is increased, which possibly participate in tumor phenotype formation (Frank et al., 2002). In embryos Brat in complex with Nanos and Pumilio work as a repressor of hunchback mRNA translation (Sonoda & Wharton, 2001).

To check the proliferative and metastatic abilities of brain tumor there was a transplantation assay carried out. The brains of *brat* mutant larvae were fragmented and transplanted into the abdominal region of adult flies-hosts. The metastatic cells were able

to proliferate and travel to distant located sites of the body including eyes, wings, legs and head. Other mutants including *lgl* and *dlg* mutants were tested in the same way, and these mutants also had the metastatic spreading (Woodhouse & Chuaqui, 1997).

1.2.2.2 *Pins* mutant neuroblasts

The protein Inscuteable (Insc) is an apically localized protein which is required for correct spindle orientation and asymmetric localization of cell fate determinants. In *insc* mutants, the spindles are misoriented from apical-basal axis, and NBs divide in random directions (Rachel Kraut *et al*, 1996; Kaltschmidt *et al*, 2000). In terms of basally distributed proteins as Numb and other cell fate determinant proteins, due to *inscuteable* mutation, they are located in random cell cortex sides. A protein called Bazooka is important for a proper functioning of Insc protein. If it is absent, Insc is located in cytoplasm and its function is disturbed.

Another protein called Pins or Partner of Inscuteable is a 70kDa protein, a GDP-dissociation inhibitor that plays a role in asymmetric cell division and mitotic spindle orientation (http://flybase.org/reports/FBgn0040080.html). It binds to Insc and is responsible for its asymmetric localization in the neuroblast. These two proteins were found to be co-dependent and absence or a mutation of any of them leads to failure in orientation of mitotic spindle as well as to defects in cell fate determinant segregation. Additionally, it was found that Pins exists in complex with heterotrimeric G protein, which also binds to Insc (Schaefer *et al*, 2000).

It was shown that in *pins* mutants, the protein inscuteable is first localized properly during NB delamination, a process, during which polarized epithelial cells detach from epithelial layer and become delaminated neuroblasts. However, during mitosis, due to *pins*

mutation, the inscuteable becomes uniformly localized in NB cytoplasm. Therefore, *pins* mutants have defective apical-basal polarity.

Moreover, Pins complex (Pins; Gαi; Dlg) also regulates cleavage furrow positioning which is important for asymmetric cell division. Basically, there are two cleavage furrow positioning pathways that work together in *Drosophila* neuroblasts: spindle-dependent pathway and cortical polarity pathway.

In the spindle-induced furrow pathway, neuroblasts set asymmetry during early prophase via localization of different proteins on apical and basal cortex. The spindle lines up with the apical/basal axis during metaphase and it becomes asymmetric during anaphase, when apical part of the spindle forms longer astral and central spindle microtubules. Consequently, the cleavage furrow is dislocated basally, producing a big apical NB and a small basal GMC.

Another cleavage furrow positioning pathway is cortical polarity dependent pathway. Cabernard et al. showed that 89% of *pins* mutant neuroblasts formed asymmetric spindle (longer in apical side) and divided asymmetrically. These neuroblasts followed the canonical spindle-induced furrow pathway. Other 11% followed cortical polarity pathway, having symmetric spindle and dividing symmetrically. These NBs had no basal cortical enrichment of furrow proteins like Pavarotti and Myosin, no basal furrow formations and daughter cells were not of different size as in spindle-dependent furrow pathway (Cabernard *et al*, 2010).

To sum up, *pins* mutant neuroblasts have defective apical basal polarity, misoriented symmetric mitotic spindle as well as symmetric cleavage furrow proteins positioning leading to symmetric NB division.

Similar to *brat* mutant brain transplantation experiment, *pins* mutant brain pieces were also implanted into the abdomen of the *Drosophila* fly to check their malignant properties. As a result, the implant showed a potential to outgrow its initial size up to 100 times, thus oversaturating the host's abdomen and killing it within two weeks. Moreover, the tumor development is not restricted to the abdominal area only, oftentimes small distant colonies consisting of immortal transformed cells are found in other tissues and organs (Caussinus & Gonzalez, 2005).

1.3 Atomic force microscopy for cell stiffness measurement

Scanning probe microscopy is a type of microscopy, where the special probe is used to scan the specimen and form the image. Atomic force microscopy (AFM) is a scanning probe microscopy having a very high resolution of less than a nanometer, which is 1000 times higher than of optical microscopy. This powerful technique can image various objects' surfaces including biological samples (e.g. cells) as well as polymers, ceramics and other material types (Sinha Ray, 2013). It is a delicate equipment that can measure different properties of the sample, including adhesion, stiffness, intracellular pressure and so on (Ludwig *et al*, 2007). AFM contains a tip of various shapes (spherical, pyramidal, conical) and sizes in nanometer scale which is attached to a cantilever. They can be made of different materials including silicon nitride (DNP-10, Bruker), diamond-like carbon (Biosphere B500-CONT, Nanotools) and others. Normally, the cantilever is coated with some reflex metals, like gold (DNP-10, Bruker) or aluminum (Respa 20, Bruker) to increase the laser signal. The cantilever indents in response to the tip-surface interaction and the resulting indentation is detected by the laser beam focused on the tip with a photodiode.

Regarding indentation, a spring constant is one of the key characteristics of the cantilever. It is affected by the length and the width of the cantilever and the material of which it is made of. The lower the spring const, the softer the cantilever is. It is important to choose a probe matching the stiffness of the sample to produce a meaningful data. For example, soft samples like cells in liquid can be scanned by probes with a low spring const (0.7 N/m and less). Another important parameter to pay attention to is a tip sharpness. When working with live cells, it is best to use tips with blunt or rounded ends in order to get a true data about their physical properties, like cell height and stiffness and not damage or kill them. (Ted F Limpoco, 2017).

AFM can be driven in different modes. Contact mode is a standard AFM mode to study the topography of various samples. When the tip and a sample are in contact or close enough the orbitals of their electrons overlay and this forms a so-called repulsive force that leads to cantilever bending. Contact mode AFM is based on measuring this force as a function of cantilever deflections. The benefit of using this mode is the resulting force is displayed directly in a raw state without system modifications. The drawback is a possible damage of soft cells and tissues due to true contact with the tip (AFM Handbook, 2018; Parksystems.com).

1.3.1 Contact mode force mapping

Force-volume mapping (contact mode force mapping) is a type of contact mode AFM measurements which is applied to obtain the map of sample physical properties in a pixel-by-pixel mode throughout the whole sample surface. It plays a significant role in studying biological samples as cells or smaller fragments and different materials as polymers (Suzuki & Mashiko, 1998).

Contact mode force mapping is a collection of all force-distance curves (Figure 4) generated at all sample points or pixels across the sample area (Radmacher *et al*, 1994).

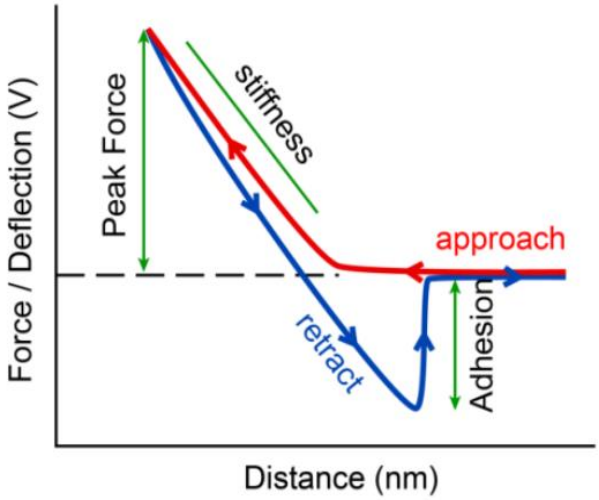

Figure 4. Force-distance curve of a typical AFM measurement point. It is usually generated during force-volume measurement. A stiffness data can be obtained from the slope of red (approach) curve. Adhesion data can be extracted from blue (retract) curve's deep region. Retrieved from T.T. Pham FDCRGP approved by Nazarbayev University.

In order to produce these graphs, the z-piezo approaches the cantilever down until it touches the surface of the sample, causing the deflection of the cantilever till the value one sets (setpoint). Each moment the tip faces the surface either of the dish or of sample, it gives the force curve, meaning that each pixel has its own data. Afterwards, the piezoelectric actuator retracts so that the probe-sample forces are broken and the feedback controller moves the probe either to x- or y-direction to repeat the measurement on the next pixel.

Since the sample surface or topography is inhomogeneous, the feedback loop is applied to balance the difference from one pixel to another. It is also responsible for sustaining the same force at each pixel (Kim et al, 2009).

1.3.2 Conversion of raw data to Young's modulus using Hertz model

AFM can generate Young's modulus (elasticity modulus) data that basically gives the information about how easily the sample can be distorted or compressed. The high values of elasticity modulus (intrinsic feature) tell about high stiffness (extrinsic feature) of the sample.

In physics Young's modulus (E) is defined as the tensile stress *(σ)* of the sample divided by the tensile strain (*ε)*. Tensile stress can be explained as a force applied per sample's unit area (*σ=F/A*), while strain is how much the sample extended per its original length (*ε=dl/l*) (https://www.birmingham.ac.uk/teachers/study-resources/stem/Physics/youngs-modulus.aspx). The unit of Young's modulus is Pascal (Pa).

$$E = \frac{\sigma}{\epsilon} = \frac{F/A}{dl/l}$$

If the sample to be studies is just pressed uniformly, its elasticity can be directly measured due to concise surface area being pressed. However, this is not the case for AFM measurements, because the surface is only indented partially with a tip having a certain shape that in complex make the indentation geometry more sophisticated. For this reason, Hertz model is applied to retrieve Young's modulus from AFM measurements, namely force-distance curves. The Young's modulus (E) can be derived from the following Hertz model formula where the spherical tip is used and indentation depth (h) is expected to be smaller than tip radius (R). P indicates the applied load and v is Poisson ratio (Kontomaris & Malamou, 2020).

$$P = \frac{4}{3}\frac{E}{1-\nu^2}R^{1/2}h^{3/2}$$

Hertz model can be applied when these assumptions are met:

- The deformations are minor (no sample cracks)

- The sample is much bigger than it's contact area with the tip
- The sample thickness is higher than the length deformed
- The sample is non-adhesive to the tip

If any of these assumptions are not met, it is possible to apply other models or corrections that can solve these issues (AFM Handbook, 2018).

Nanomechanical investigation of cells is attaining higher importance these days in several areas like cancer and developmental biology. The contrasts in stiffness of normal and cancer cells were revealed. Conjointly, it was found that the diminished cell stiffness can alter the metastatic potential of the malignant cell (Denitsa Docheva, 2008). In developmental biology, the study of cell cortex tension of zebrafish germ layer progenitors showed that the ecto-, meso- and endodermal progenitor cells were different in terms of cell stiffness (Krieg *et al*, 2008). Another case is the mechanical study of growth substrates. It revealed that the appropriate stiffness or elasticity of the matrix is crucial for the stem cell differentiation and cell lineage specification (Engler *et al*, 2006). Apart from the cells and tissues, the fibers as representatives of the extracellular matrix were also nanomechanically investigated (Wenger *et al*, 2007). The AFM capabilities are used not only in biophysical studies, but also to study the elasticity of various materials and matrices (Touhami *et al*, 2003).

2 MATERIAL AND METHODS

2.1 Reagents and media for live cell imaging

Table 1. The compositions of Schneider insect medium and Chan & Gehring solution

A

Components	mg/L
Glycine	250.0
L-Arginine	400.0
L-Aspartic acid	400.0
L-Cysteine	60.0
L-Cystine	100.0
L-Glutamic acid	800.0
L-Glutamine	1800.0
L-Histidine	400.0
L-Isoleucine	150.0
L-Leucine	150.0
L-Lysine hydrochloride	1650.0
L-Methionine	800.0
L-Phenylalanine	150.0
L-Proline	1700.0
L-Serine	250.0
L-Threonine	350.0
L-Tryptophan	100.0
L-Tyrosine	500.0
L-Valine	300.0
Beta-Alanine	500.0
Calcium Chloride (CaCl2) (anhyd.)	600.0
Magnesium sulfate (MgSO4) (anhyd.)	1806.9
Potassium chloride (KCl)	1600.0
Potassium phosphate monobasic	450.0
Sodium bicarbonate (NAHCO3)	400.0
Sodium chloride (NaCl)	2100.0
Sodium phosphate dibasic anhydrous	701.1
Alpha-Ketoglutaric acid	200.0
D-Glucose (Dextrose)	2000.0
Fumaric acid	100.0
Malic acid	100.0
Succinic acid	100.0
Trehalose	2000.0
Yestolate	2000.0

+1% FBS

B

Components	mg/L
NaCl	3200.0
KCl	3000.0
CaCl2*2H2O	690.0
MgSO4*7H2O	3700.0
Tricine buffer (pH 7)	1790.0
Glucose	3600.0
Sucrose	17100.0
+ Bovine serum albumin (BSA, fraction V)	1000.0

A. Schneider insect medium (S2) composition (Schneider, 1964). B. Chan & Gehring solution composition (Chan & Gehring, 1971).

Table 2. Enzymes used in primary culture preparation

Enzyme	Concentration	Company
Papain	10 mg/ml dissolved in CGS	Sigma
Collagenase type I	10 mg/ml dissolved in CGS	Sigma

2.2 *Drosophila* transgenic lines used in this project

All fly stocks were kept in the plastic vials with fly food in the incubator with a set temperature of 18°C. The flies used for experiments were maintained at 25°C in a separate incubator. In order to produce a mutant larvae, pre-selected males and virgin females were crossed in the vial and kept at 25°C. The newly hatched virgins of female flies were added every day when needed as well as male flies. As a rule, every 1-2 weeks the adult flies were replaced by a younger generation to maintain the sustainable reproduction.

Fly stocks used in this project are listed in table 3 and the *Drosophila* lines used for live cell imaging and AFM measurements can be found in table 4.

All flies used in the experiments are transgenic having fluorescent tag on proteins as Sqh::EGFP (non-muscle myosin II regulatory light chain (Karess *et al*, 1991)), Cherry::Zeus (mitotic spindle marker (Mauri *et al*, 2014)) and Caax::Cherry (cell membrane protein (Manolaridis *et al*, 2013)).

Transgenic lines were generated by PCR amplification of synthesized oligonucleotides/sequences followed by in-fusion technology (Takara, Clontech) which allows to clone the gene of interest into a plasmid-vector. Then these vectors were injected into flies for targeted insertion on 2^{nd} or 3^{rd} chromosome (Pham *et al*, 2019).

Transgenes expression is done via driver gene worGal4 which is specific to neuroblasts (Albertson & Doe, 2003). UAS is a regulatory region or effector, to which worGal4 can bind and drive the expression of fluorescent proteins. (http://flybase.org/reports/FBtp0040573.html)

Table 3. Transgenic fly stocks

Wildtype (wt)	w⁻;worGal4,Sqh:EGFP,UASCherry:Zeus/CyO; UASCaax:Cherry/TM6B	(Cabernard *et al*, 2010)
Pins^{P62}	w⁻;UASCaax:Cherry/CyO;Pins^{P62}/TM6B	(Yu *et al*, 2000)
Pins^{P89}	w⁻;worGal4,Sqh:EGFP,UASCherry:Zeus/CyO; Pins^{P89}/TM6B	(Yu *et al*, 2000)
Brat	w⁻;UASBratRNAi/CyO;MKRS/TM6B	(Harris *et al*, 2011)

Drosophila pins mutant lines were generated according to protocol (Yu et al, 2000). P(w+) transposon, EP3559 (Rorth, 1996)was inserted at cytological location 98A-B, ~700 bp 5′ upstream to the pins cDNA. It was mobilized with the P[ry+ δ2-3](99B) immobile element as a transposase source. As a result, small deletions were generated which partially removed *pins* coding region. This way, *pins*^{P89} and *pins*^{62} loss of function alleles were produced.

On the other hand, *brat* mutant flies were generated by site-directed mutagenesis using QuikChange (Stratagene) (Harris *et al*, 2011).

Table 4. Transgenic fly lines used for experiments

wildtype	w⁻;worGal4,Sqh:EGFP,UASCherry:Zeus/CyO; UASCaax:Cherry/TM6B
♀*Brat* virgin	w⁻;UASBratRNAi/CyO;MKRS/TM6B
♂ wt	w⁻;worGal4,Sqh:EGFP,UASCherry:Zeus/CyO; UASCaax:Cherry/TM6B
Product of cross (*Brat* mutant)	w⁻;UASBratRNAi/worGal4,Sqh:EGFP,UASCherry:Zeus;UASCaax:Cherry/MKRS and w⁻;UASBratRNAi/worGal4,Sqh:EGFP,UASCherry:Zeus;UASCaax:Cherry/TM6B
♀ *Pins*^{P62} virgin	w⁻;UASCaax:Cherry /CyO; Pins^{P62}/TM6B
♂ *Pins*^{P89}	w⁻;worGal4,Sqh:EGFP,UASCherry:Zeus/CyO; Pins^{P89}/TM6B
Product of cross (*Pins* mutant)	w⁻;worGal4,Sqh:EGFP,UASCherry:Zeus/UASCaax:Cherry;Pins^{P62}/ Pins^{P89}

2.3 Live cell imaging

I used the following standard live cell imaging protocol (Cabernard & Doe, 2013):

The fly adults were crossed in the plastic vial containing fly food and incubated at 25°C for 1 day. The next day adults were taken out from the vial so that the eggs laid were of the same age. When the larvae were 72-96 hours old, they were dissected and used for live cell imaging.

Drosophila melanogaster 3rd instar larvae were dissected at a room temperature in Schneider insect medium (S2 medium) + 1% Fetus Bovine Serum (FBS) using ZEISS stereoscope. About 8-10 intact brains were collected and stored in μ-slide angiogenesis (ibidi) and aligned with anterior surface down. The imaging was initially performed using ZEISS LSM 980 Airyscan 2 confocal microscope and later was substituted by Leica Thunder Imager due to technical problems of the first microscope. The images were acquired with 100x/1.4 immersion oil objective on Leica microscope and 100x/1.46 objective on ZEISS LSM980. The images were taken every 15 seconds for mitosis time and every 1 min for cell cycle time measurements. The z-step size was 1.25 um and the stack consisted of 20-30 slices.

In order to compare S2 medium and CGS we implemented the similar protocol replacing S2 medium + 1% FBS to Chan & Gehring solution.

2.4 Primary culture of post-embryonic *Drosophila* neuroblasts

To prepare the primary NBs culture of *Drosophila melanogaster* I followed an existing protocol (Berger *et al*, 2012) with few modifications: the brains were washed and dissociated in CGS, instead of S2 (Marques *et al*, 2021).

About 20-30 larvae of 72-96 hours age were picked from the vial with fly food and surface sterilized by washing twice in sterile water, twice in ethanol (for 30 sec each) and again twice in sterile water. The larvae were dissected in CGS at room temperature for no more than 30 minutes. The brains were collected in a separate well containing 400 ul of CGS. Then 50 ul of collagenase I in and 50 ul of papain (Table 2) were added, then the well was covered with parafilm and was incubated at 30°C for about 30-40 minutes. After, brains were gently washed with CGS and 400 ul of this media containing brains were transferred into 1.5 ml Eppendorf tube to be dissociated with 200 ul tip by slow pipetting the solution until it was homogenized. After that, the dissociated brains were plated on TPP dish and settled for about 20 minutes which was followed by addition of another 1ml CGS of room temperature on top.

2.5 Cortical stiffness measurements using AFM

The primary neuroblast cultures of 3rd instar larvae were employed to study the cell stiffness using NanoWizard 4 XP AFM coupled to ZEISS Observer microscope. All of the experiments were performed in liquid (CGS) using contact mode force mapping regime. The TPP dish with primary culture of neuroblasts was placed on AFM stage that was fixed on the microscope. The 20x/0.4 objective was used to visualize the cells to be measured as well as Dino-lite edge digital camera was used to align the laser on cantilever and reach the maximal signal. The probe with a nominal spring const (k) of 0.2 N/m and the spherical tip radius 500 nm (B500-CONTR, Nanoandmore, Germany) was used to measure the cortical stiffness of neuroblasts of interphase stage. The scan size used was 15-20 um with 1um pixel size. The force applied was 0.2 nN for wildtype and mutant

lines. The extension speed or z-speed was set to 20 um/s and z-length or extension length was 3-5 um for *pins* mutant and 5-8 um for wildtype and *brat* mutant neuroblasts.

2.6 The analysis and quantification

2.6.1 Image analysis for live cell imaging data

All images were analyzed using Imaris software. The slice mode or oblique slicer were used to find the best view for a certain cell to calculate its mitosis or cell cycle time. For measuring the cell size, we produced one single image per each cell with the biggest area of the cell aligned with its spindle on Imaris software by crop 3D, crop time, delete slices functions. These images were further modified on Image J in order to draw cells' boundaries and after the cross-sectional area of the neuroblasts were calculated by a custom-made MatLab code written by our Principal Investigator- Dr. Tri Pham. The last step was to multiply the resulting area numbers to X-voxel and Y-voxel values for each individual cell. The spindle length was measured directly on Imaris software.

2.6.2 Cortical stiffness quantification

JPK Data Processing software was used to analyze the stiffness data. The Hertz fit was applied in order to extract the Young's modulus of the sample studied. Each pixel of the scan generates the force-distance curve, the slope of the linear part of these graphs gives the data about the stiffness. We used stiffness image in parallel with height image in order to obtain the stiffness data from 3x3 pixels of the highest part of the cell. The selected pixels of the slope (stiffness) image display the average value of Young's modulus in Pascals.

2.6.3 Replicates and statistical analysis

The statistical analyses were made with GraphPad Prism. Each experiment's data is generated from at least 3 independent experiments. The minimum of 5 larvae were dissected per each individual experiment. Two-tailed t-test was used to compare two samples with equal variances and show whether there was a statistically significant difference between two groups. For two groups with different variances Welch's correction t-test was applied. Mann-Whitney test was used as a non-parametric test for not normally distributed samples.

The asterisk depicted on the graphs represent different statistical significances:

*; $p < 0.05$, **; $p < 0.01$, ***; $p < 0.001$, ****; $p < 0.0001$, ns; not significant.

3 AIM OF THE THESIS PROJECT

Research question: Is there a clear difference in the biophysical and biomechanical properties between normal and cancer neural stem cells?

Hypothesis: Normal neural stem cells have different biophysical and biomechanical properties to cancer neural stem cells.

Aim: To systematically characterize the biophysical and biomechanical properties of normal and cancer neural stem cells.

4 RESULTS

4.1 Cell cycle and mitosis times of *Drosophila* neuroblasts are different in Schneider insect medium and Chan & Gehring solution

Schneider insect medium or S2 is a standard solution used for live cell imaging of *Drosophila* larval neuroblasts (Schneider, 1964). Chan & Gehring solution on the other hand is a standard solution used for preparation of neuroblast primary cultures (Chan & Gehring, 1971). Due to shipping complications to Kazakhstan and complex composition of S2 medium (Table 1A) as well as its high price and contrasting cheaper CGS with simpler composition (Table 1B) that can be easily prepared fresh from powders directly in the lab, we decided to compare CGS' and Schneider medium's effects on *Drosophila* neuroblast division in terms of mitosis time and cell cycle time. Both mitosis and cell cycle times are calculated based on 3 observable timepoints of neuroblast cell division: nuclear envelope breakdown, anaphase onset and complete cytokinesis (Figure 5).

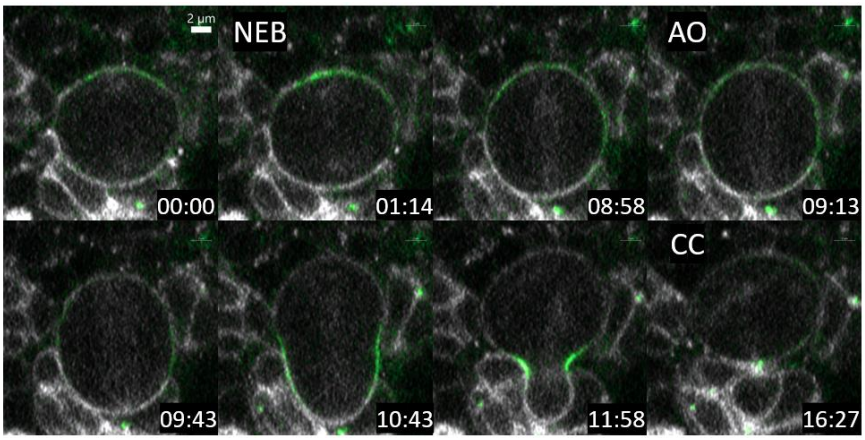

Figure 5. Image sequence of asymmetrically dividing wildtype neuroblast. Cell membrane and spindle (white), non-muscle myosin II (green). NEB- nuclear envelope breakdown, AO- anaphase onset, CC- complete cytokinesis. The scale bar is 2 um. Time is shown as a minute : second from prophase.

Nuclear envelope breakdown (NEB) (Figure 5) takes place during prophase and can be observed at the moment when the two centrosomes form the spindle for the first time

indicating the nuclear envelope disappearance. Anaphase onset (AO) is a time point denoting the initiation of anaphase and it is observed when the spindles pull apart for the first time. Complete cytokinesis (CC) is the last time point of cell division, it indicates the end of telophase and can be observed when the constriction ring closes completely.

Mitosis time is a time interval between two defined mitotic stages during one division. It can be calculated as a time between NEB and AO, or AO to CC or NEB to CC. In this project, all three mitosis times were measured.

Cell cycle time, on the other hand, is a time difference between exactly the same mitotic stages of divisions 1 and 2. In this project, all cell cycle times were calculated based on complete cytokinesis stage:

CC (2^{nd} cycle) – CC (1^{st} cycle) = cell cycle time

To learn how different media effect neuroblast cell cycle and mitosis times, we performed live cell imaging of 3^{rd} instar larval neuroblasts of three different transgenic fly strains: wildtype, *brat* mutant and *pins* mutant (Figure 6) in CGS and S2.

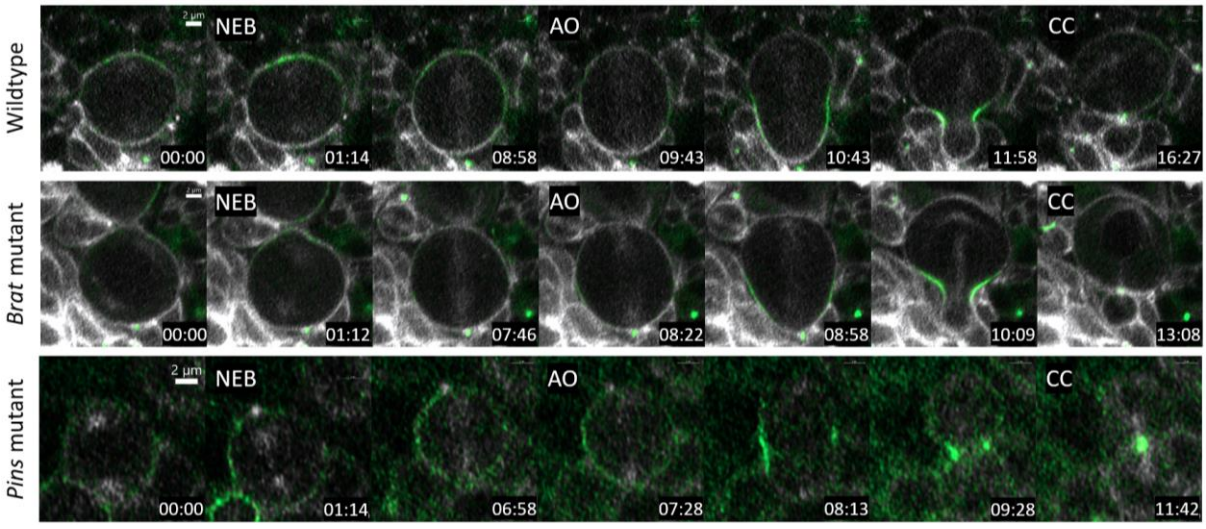

Figure 6. Sequence images of asymmetrically dividing wildtype and *brat* mutant neuroblasts and symmetrically dividing *pins* mutant neuroblast. Cell membrane and spindle (white), non-muscle myosin II (green). NEB- nuclear envelope breakdown, AO- anaphase onset, CC- complete cytokinesis. The scale bar is 2 um. Time is shown as a minute : second from prophase.

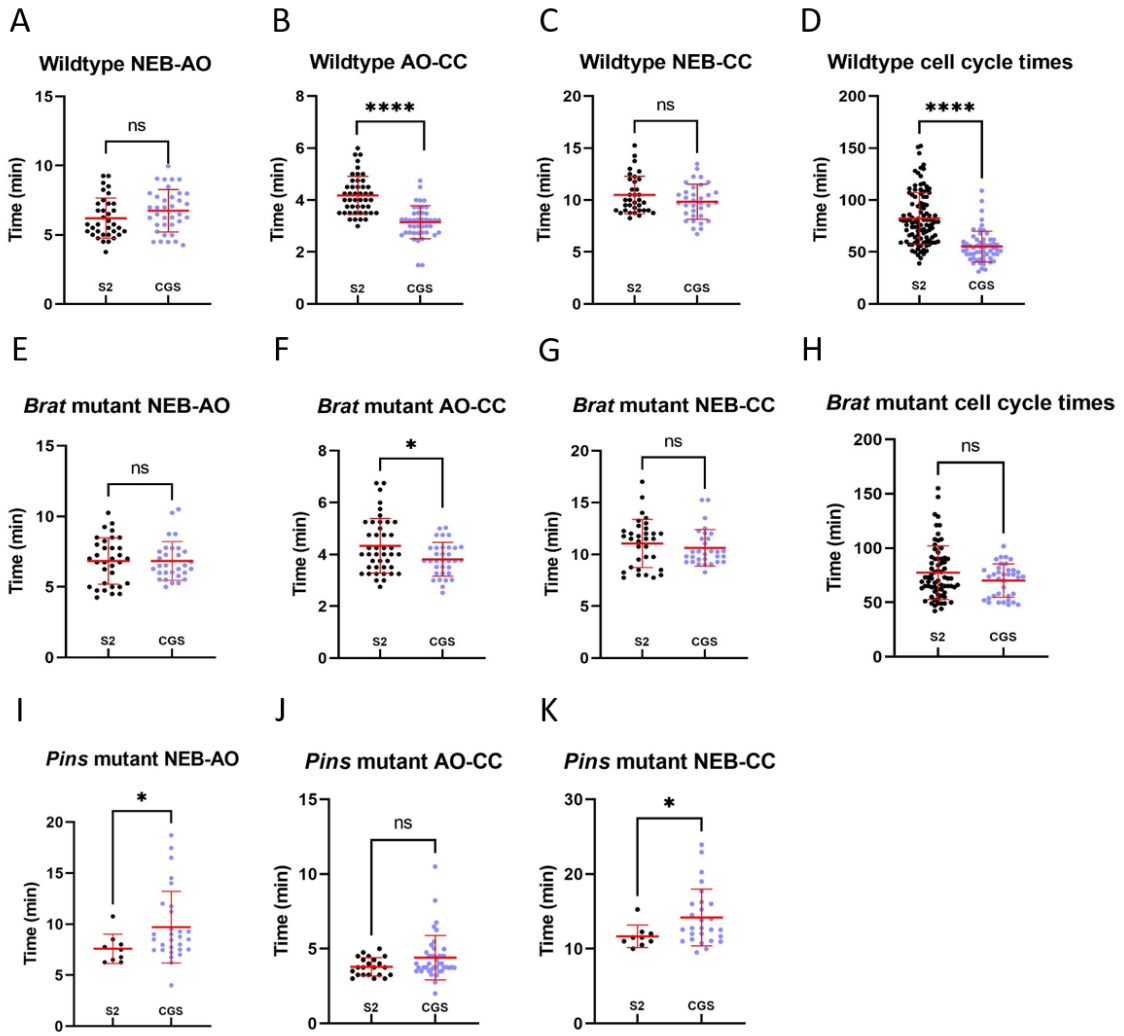

Figure 7. The cell cycle and mitosis times of *Drosophila* neuroblasts are different in Schneider insect medium and Chan & Gehring solution. Wildtype neuroblasts mitosis times from NEB to AO (A), AO to CC (B) and NEB to CC (C) are compared for S2 (black) and CGS (purple), respectively. Similar measurements were done for *brat* mutant (E, F, G) and *pins* mutant (I, J, K) neuroblasts. Cell cycle times in two media are compared for wildtype (D) and *brat* mutant (H) NBs. Mean and SD are indicated in red. Each dot represents an individual cell.

Overall, there was no difference between mitosis times of wildtype neuroblasts in CGS and S2 medium (Figure 7C). However, particularly at AO-CC mitosis times, wildtype neuroblast constricted faster in CGS (Figure 7B). Figure 7D clearly shows that in CGS wildtype neuroblasts divided faster. In the case of *brat* mutant neuroblasts, CGS and S2 medium had the same effect on the cell division behavior, except for AO-CC mitosis

times being faster in CGS (Figure 7F). On the other hand, the mitosis time of *pins* mutant neuroblasts was longer in CGS, than in S2 medium (Figures 7I and K).

4.2 *Brat* mutant neuroblasts divide longer than wildtype in CGS, but not in S2 medium

We took cell cycle time measurements as one of the parameters to study the differences between normal and cancer neural stem cells. In figure 8, *brat* mutant neuroblasts cell cycle times are compared to wildtype in two different media. According to standard media (S2), there is no statistically significant difference between two lines. However, in experimental CGS *brat* mutant NBs divide longer than wildtype. The generation of cell cycle times data for *pins* mutant NBs was not possible, because once these NBs divide symmetrically, they produce two GMCs and zero self-renewed neuroblast (Lee *et al*, 2006a). Therefore, we could not observe second division of *pins* mutant neuroblasts to calculate their cell cycle time.

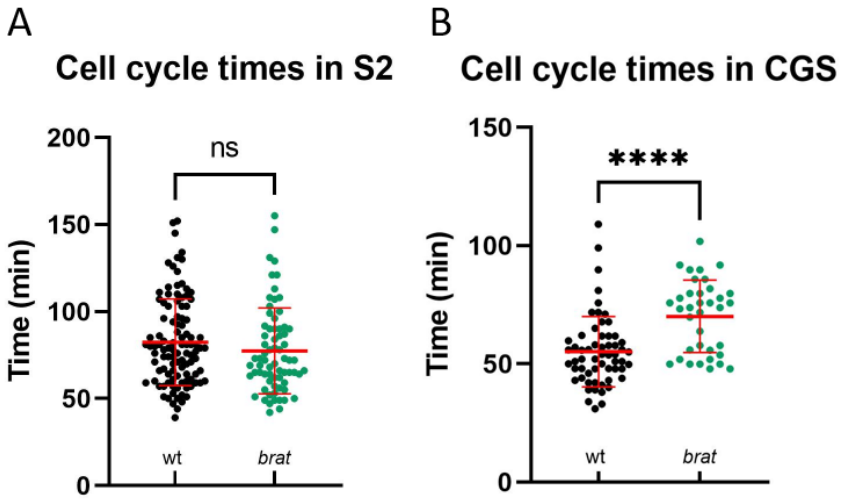

Figure 8. *Brat* mutant neuroblasts divide longer than wildtype in CGS, but not in S2 medium. Cell cycle times comparisons of wildtype (black) and *brat* mutant neuroblasts (green) are shown in S2 (A) and in CGS (B). Mean and SD are indicated in red. Each dot represents an individual cell.

4.3 *Pins* mutant neuroblasts divide longer than wildtype and *brat* mutant neuroblasts only in CGS, but not S2 medium

Next, we compared wildtype, *brat* mutant and *pins* mutant neuroblasts based on their mitosis times (Figure 9). In Schneider's insect medium, *brat* mutant neuroblasts didn't show any difference from wildtype NBs. *Pins* mutant NBs were neither dramatically different from wildtype, as AO-CC and NEB-CC mitosis times were similar for both. When the mitosis times for normal and cancer neural stem cells were measured in CGS, the results came up differently. Here, *brat* mutant NBs division from anaphase onset till complete cytokinesis (AO-CC) was significantly longer than in wildtype, while keeping the similarity to normal cell division in other stages of mitosis. *Pins* mutant NBs, which had almost no difference from wildtype in S2 medium, divided significantly longer in CGS at all stages of mitosis.

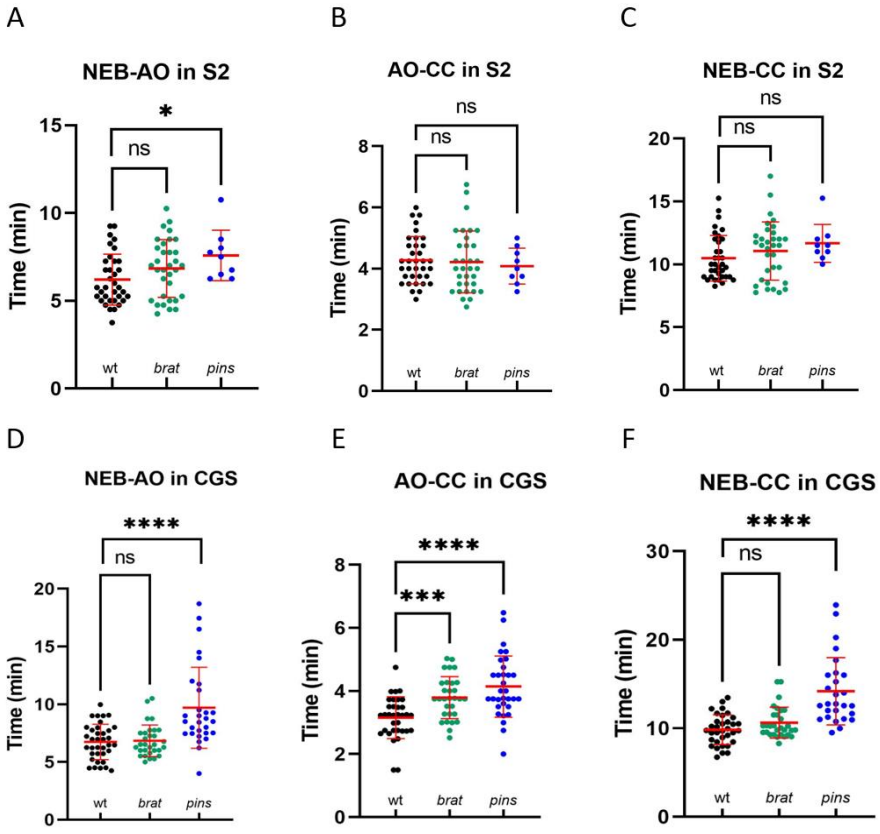

Figure 9. *Pins* mutant neuroblasts divide longer than wildtype in CGS. Wildtype (black), *brat* mutant (green) and *pins* mutant (blue) neuroblasts' NEB-AO, AO-CC, NEB-CC mitosis times in S2 medium are shown in A, B, C, respectively. D, E, F. Mitosis times of three lines represented are in CGS. Mean and SD are indicated in red. Each dot represents an individual cell.

4.4 *Pins* mutant neuroblasts have shorter spindle length and smaller cross-sectional area in contrast to wildtype

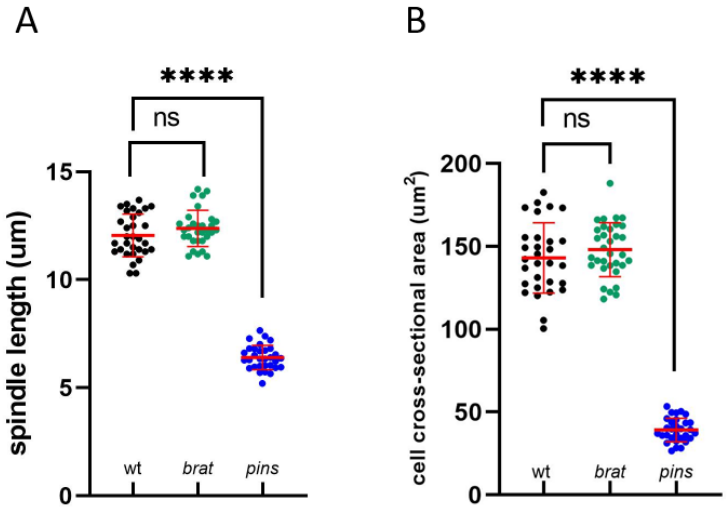

Figure 10. *Pins* mutant neuroblasts have shorter spindle length and smaller size in contrast to wildtype neuroblasts. Spindle lengths (A) and cell cross-sectional area (B) of wildtype (black), *brat* mutant (green) and *pins* mutant (blue) NBs are shown. Mean and SD are indicated in red. Each dot represents an individual cell.

Other parameters employed to check the differences between cancer and normal cells were cross-sectional area of the cell and the spindle length. An average of spindle length of normal NBs was about 12 micrometers, for *brat* mutant NBs' mean was about 12.4, therefore they are considered as similar. In contrast, *pins* mutant NBs had spindle length of 6.4 um in average, which is almost twice less than of wildtype and *brat* mutant neuroblasts (Figure 10A).

In terms of cell cross-sectional area, the trend is the same, where *pins* mutant neuroblasts are much smaller than the NBs of other two (Figure 10B).

4.5 *Pins* mutant neuroblasts are softer than wildtype neuroblasts

To test if there is a difference between wildtype and mutants based on the stiffness, we used atomic force microscopy. The primary cultures were used as a sample for AFM measurements, instead of intact brains, as in previous experiments.

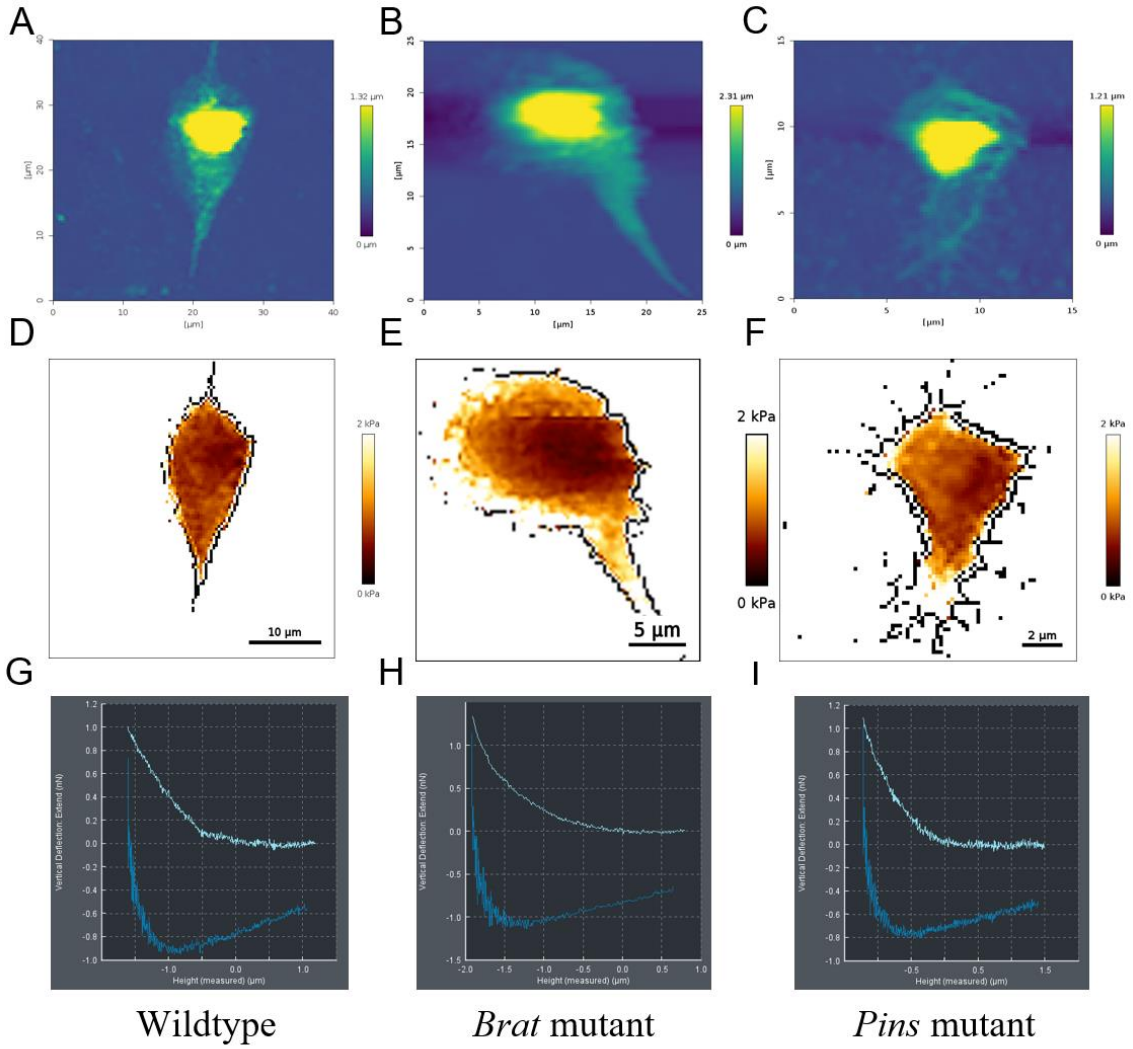

Figure 11. The representative images of wildtype, *brat* and *pins* mutant isolated neuroblasts generated by AFM. A. B. C. The AFM generated height data of wildtype, *brat* mutant and *pins* mutant isolated neuroblasts, respectively, yellow color indicates higher region. Stiffness data is shown in D.E.F., where the darker brown color shows the softer region. G.H.I. The representative force-distance curves generated from one pixel of the highest regions of the cells.

The Young's moduli of three different neuroblast strains were measured and compared. We revealed that *pins* mutant neuroblasts are softer than wildtype neuroblasts, whereas

there was no statistically significant difference between wildtype and *brat* mutant NBs (Figure 12).

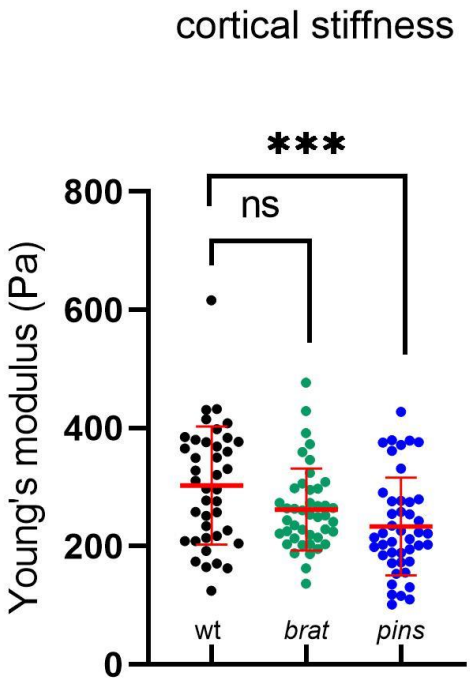

Figure 12. *Pins* mutant neuroblasts are softer than wildtype. The Young's modulus values are shown for wildtype (black), *brat* mutant (green) and *pins* mutant (blue) isolated neuroblasts. Mean and SD are indicated in red. Each dot represents an individual cell.

5 DISCUSSION

5.1 Cell cycle and mitosis times of *Drosophila* neuroblasts are different in Schneider insect medium and Chan & Gehring solution

As it was mentioned, based on the lower price of CGS and relative easiness of its preparation in the lab, we decided to compare cell cycle and mitosis times of wildtype, *brat* and *pins* mutants neuroblasts in CGS to that of S2. The absence of statistically significant difference between them would give us the basis to replace S2 by CGS. However, the results came up opposite. The mitosis times of both *brat* mutant and wildtype in different media showed that AO-CC mitosis times, the time periods between the cell splitting initiation and final constriction, were faster in CGS, than in S2 medium. Additionally, the wildtype neuroblasts divided faster in CGS, in contrast to S2 medium, according to their cell cycle times comparison graph (Figure 7D). This trend might be because of the higher glucose concentration in CGS than in S2 medium (Table 1). It is well-known that the glucose is the source of energy which is required for cell fundamental processes as growth and division (Yuan *et al*, 2013). Moreover, the correlation between the glucose content and cancer cell proliferation was shown to be directly proportional (Han *et al*, 2015).

On the other hand, *pins* mutant neuroblasts showed the contradictory result, where the cells' mitosis time was longer in CGS, than in S2. It is possible that these cells require higher amount of amino acids present in S2 to maintain a sustainable growth.

5.2 *Brat* mutant neuroblasts divide longer than wildtype in CGS, but not in S2 medium

The comparative analysis of cell cycle times of wildtype and *brat* mutant neuroblasts in S2 medium revealed that they are non-significantly different. This is an interesting observation, that can be explained by the nature of Brat protein function. The Brat is a protein that segregates into the INP (type II NBs) because of its basal localization and it functions as a cell fate determinant to cause the further differentiation. It means that the mutation of the *brat* gene causes the changes not in the neuroblast itself, but in INP behavior. Therefore, *brat* mutant neuroblasts might behave similar to wildtype, whereas mutant INP can demonstrate altered properties when compared to its wildtype analog.

The cell cycle times comparison in CGS, on the other hand, showed that *brat* mutant neuroblasts divide longer than wildtype. It is another result proving that CGS and S2 media act differently on normal and cancer cells. Possible explanation for different results obtained from two different solutions is that S2 medium provides essential amino acids required for normal cell behavior (growth and proliferation), while CGS is a basic salt buffer, which may affect the proliferation rate and division time of normal and cancer NBs.

5.3 *Pins* mutant neuroblasts divide longer than wildtype and *brat* mutant neuroblasts only in CGS, but not S2 medium

The standard solution, S2, showed not much significant difference between mitosis times of all three fly lines. The *pins* mutant neuroblasts divided longer in NEB-AO mitosis time in contrast to wildtype, but in total there was no difference between these lines. The

absence of difference between mitosis times of wildtype and *pins* mutant cells might be because of small sample size of *pins* mutant NBs, which was due to time limitations and very low number of NBs in these mutant brains.

When imaged in CGS, *pins* mutant NBs divided longer than wildtype, while *brat* mutant neuroblasts took approximately the same amount of time to split. A significant difference between *pins* mutant and normal NBs division might be explained based on the fact that Pins is an apically localized protein that directly affects the neuroblast and its mutation leads to several joint consequences as symmetric distribution of non-muscle myosin II, defective apical-basal polarity and spindle orientation. Hence, the *pins* mutant neuroblasts, here, is possibly assumed as a true neuroblast mutant, and if so, it is logically correct, that mutants might require more time to divide because of their abnormalities. However, as mentioned in paragraph 5.2, the different results observed in two media might be because of possible disturbance of proliferation rates in CGS.

5.4 *Pins* mutant neuroblasts have shorter spindle length and smaller cross-sectional area in contrast to wildtype

The NBs' largest cross-sectional area and a spindle length at the biggest slice were measured and compared for three lines. It turned out that NBs with *pins* mutation are 3.5 times smaller than healthy cells in cross-sectional area. The size difference is related to the mode of division. Wildtype and *brat* mutant NBs divide asymmetrically, producing one large neuroblast and a smaller progenitor cell. It was found that after each asymmetric division larval neuroblasts grow back to their pre-division size (Carmena, 2018), that in turn gives the potential to divide more (up to 100 times). Whereas *pins* mutant NBs divide symmetrically giving rise to two identical cells. It was shown that these NBs fail to self-

renew and the daughter cells produced are GMCs (Lee et al, 2006a). Another study proved that *pins* mutant NBs do not produce two neuroblasts as a result of symmetric division, since no such overgrowth was observed as well as the brain size was not enlarged (Zhang *et al*, 2016). Therefore, the symmetric division of NB observed might be its last division. This can explain the smaller size of *pins* mutant NBs in comparison to other two strains, as the size of NBs dividing the last time is always smaller than the size of NBs dividing for the first times.

However, it is not clear what cells cause cancer in host flies when *pins* mutant brains are transplanted. As mentioned, besides symmetrically dividing NBs that we studied, there are also asymmetrically dividing neuroblasts in *pins* mutant brains. Therefore, it is possible that these NBs not covered in this project are the cause of tumorigenesis.

5.5 *Pins* mutant neuroblasts are softer than wildtype neuroblasts

The last biomechanical property compared between three strains of *Drosophila melanogaster* was cortical stiffness measurements on AFM. The primary cultures of wildtype, *brat* mutant and *pins* mutant neuroblasts were tested and the statistical analysis indicated that *pins* mutant NBs have the lowest Young's modulus, which means that these are the softest cells among others. We expected that mutant NBs might have lower stiffness than normal analogs, because both mutant lines were proven to act like cancer cells and it is known that soft cells can move easier and form metastases, for example. Again, *brat* mutant had no difference from wildtype NBs. However, it is possible that *brat* mutant progenitor cells had altered stiffness compared to wildtype GMC or INP, and it is a potential future research project to test their differences.

5.6 Limitations

For AFM measurements we used primary neuroblast cultures, meaning that cell-cell adhesion influences that are naturally present in intact brains were neglected. Additionally, stiffness data of some cell's pixels might contain not pure cortical stiffness, but a combination with nuclear stiffness, since the distance between the nucleus and the cell cortex may vary depending on interphase stage and the entire range of measurements were selected during data processing, instead of a curve portion containing the data about cortical stiffness only. Due to time limitations and very low number of neuroblasts in *pins* mutant brains, the statistics on mitosis time of this mutant line in S2 was produced based on 9 cells only. Lastly, we had no fly lines with markers distinguishing type I from type II NBs.

6 CONCLUSIONS

6.1 Conclusions

The objective of this project was to identify the differences between healthy and cancer cells by comparing their biophysical and biomechanical properties such as: cell cycle time, mitosis time, cell size, spindle length and cortical stiffness. Based on our current findings, we made the following conclusions. First, there is no difference in the biophysical and biomechanical properties between *brat* mutant and wildtype NBs. Whereas *pins* mutant NBs showed differences in many of the properties tested. It turned out that mitosis time of *pins* mutant NBs is similar to wildtype in S2, however it is higher in CGS. Additionally, *pins* mutant neuroblasts were found to be softer and smaller in size compared to wildtype NBs. Overall, we think that depending on the type of cancer or mutation, the cells may display different biophysical and biomechanical properties in contrast to wildtype NBs. It is also interesting to note that depending on the culture medium (S2 medium or CGS) the cell cycle and mitosis times can change due to their differences of nutritional values.

6.2 Future directions

We have only measured and compared the cortical stiffness of normal and cancer neural stem cells. One of the future directions is to measure and compare the nuclear stiffness of normal and cancer NBs by treating them with latrunculin A (Fischer *et al*, 2020) to remove the actin cytoskeleton. Furthermore, we can check the differences between cortical and nuclear stiffness of healthy and mutant (*brat*) INPs or GMCs for type II NBs.

Additionally, we will have to measure the biophysical properties of asymmetrically dividing *pins* mutant NBs.

7 REFERENCE LIST

Abidine Y, Constantinescu A, Laurent VM, Sundar Rajan V, Michel R, Laplaud V, Duperray A & Verdier C (2018) Mechanosensitivity of Cancer Cells in Contact with Soft Substrates Using AFM. *Biophysical Journal* 114: 1165–1175

Albertson R & Doe CQ (2003) Dlg, Scrib and Lgl regulate neuroblast cell size and mitotic spindle asymmetry. *Nature Cell Biology* 5: 166–170

Arama E, Dickman D, Kimchie Z, Shearn A & Lev Z (2000) Mutations in the b-propeller domain of the Drosophila brain tumor (brat) protein induce neoplasm in the larval brain

Bellen HJ, Levis RW, Liao G, He Y, Carlson JW, Tsang G, Evans-Holm M, Hiesinger PR, Schulze KL, Rubin GM, *et al* (2004) The BDGP gene disruption project: Single transposon insertions associated with 40% of Drosophila genes. *Genetics* 167: 761–781

Bello BC, Izergina N, Caussinus E & Reichert H (2008) Amplification of neural stem cell proliferation by intermediate progenitor cells in Drosophila brain development. *Neural Development* 3: 5

Berger C, Harzer H, Burkard TR, Steinmann J, van der Horst S, Laurenson AS, Novatchkova M, Reichert H & Knoblich JA (2012) FACS Purification and Transcriptome Analysis of Drosophila Neural Stem Cells Reveals a Role for Klumpfuss in Self-Renewal. *Cell Reports* 2: 407–418

Betschinger J, Mechtler K & Knoblich JA (2006) Asymmetric Segregation of the Tumor Suppressor Brat Regulates Self-Renewal in Drosophila Neural Stem Cells. *Cell* 124: 1241–1253

Blackadar CB (2016) Historical review of the causes of cancer. *World Journal of Clinical Oncology* 7: 54–86 doi:10.5306/wjco.v7.i1.54 [PREPRINT]

Boone JQ & Doe CQ Identification of Drosophila Type II Neuroblast Lineages Containing Transit Amplifying Ganglion Mother Cells.

Bowman SK, Rolland V, Betschinger J, Kinsey KA, Emery G & Knoblich JA (2008) The Tumor Suppressors Brat and Numb Regulate Transit-Amplifying Neuroblast Lineages in Drosophila. *Developmental Cell* 14: 535–546

Brand H & Perrimon N (1993) Targeted gene expression as a means of altering cell fates and generating dominant phenotypes

Butcher DT, Alliston T & Weaver VM (2009) A tense situation: Forcing tumour progression. *Nature Reviews Cancer* 9: 108–122 doi:10.1038/nrc2544 [PREPRINT]

Cabernard C & Doe CQ (2009) Apical/Basal Spindle Orientation Is Required for Neuroblast Homeostasis and Neuronal Differentiation in Drosophila. *Developmental Cell* 17: 134–141

Cabernard C & Doe CQ (2013) Live imaging of neuroblast lineages within intact larval brains in Drosophila. *Cold Spring Harbor Protocols* 2013: 970–977

Cabernard C, Prehoda KE & Doe CQ (2010) A spindle-independent cleavage furrow positioning pathway. *Nature* 467: 91–94

Carmena A (2018) Compromising asymmetric stem cell division in Drosophila central brain: Revisiting the connections with tumorigenesis. *Fly (Austin)* 12: 71–80

Carmena A (2020) Molecular Sciences The Case of the Scribble Polarity Module in Asymmetric Neuroblast Division in Development and Tumorigenesis.

Caussinus E & Gonzalez C (2005) Induction of tumor growth by altered stem-cell asymmetric division in Drosophila melanogaster. *Nature Genetics* 37: 1125–1129

Chan L-N & Gehring W (1971) Determination of Blastoderm Cells in Drosophila melanogaster (imaginal discs/insect embryo/cell culture/differentiation/determinative factors)

Chaudhuri O, Cooper-White J, Janmey PA, Mooney DJ & Shenoy VB (2020) Effects of extracellular matrix viscoelasticity on cellular behaviour. *Nature* 584: 535

Choksi SP, Southall TD, Bossing T, Edoff K, de Wit E, Fischer BEE, van Steensel B, Micklem G & Brand AH (2006) Prospero Acts as a Binary Switch between Self-Renewal and Differentiation in Drosophila Neural Stem Cells. *Developmental Cell* 11: 775–789

Connell M, Cabernard C, Ricketson D, Doe CQ & Prehoda KE (2011) Asymmetric cortical extension shifts cleavage furrow position in Drosophila neuroblasts. *Molecular Biology of the Cell* 22: 4220–4226

Couturier L, Mazouni K & Schweisguth F (2013) Numb localizes at endosomes and controls the endosomal sorting of notch after asymmetric division in drosophila. *Current Biology* 23: 588–593

Cross SE, Jin YS, Rao J & Gimzewski JK (2007) Nanomechanical analysis of cells from cancer patients. *Nature Nanotechnology* 2: 780–783

Denitsa Docheva (2008) Researching into the cellular shape, volume and elasticity ofmesenchymal stem cells, osteoblasts and osteosarcoma cellsby atomic force microscopy.

Diganta Dutta, Xavier-Lewis Palmer, Jose Ortega-Rodas, Vasundhara Balraj, Indrani Ghosh Dastider & Surabhi Chandra (2020) Biomechanical and Biophysical Properties of Breast Cancer Cells Under Varying Glycemic Regimens.

Engler AJ, Sen S, Sweeney HL & Discher DE (2006) Matrix Elasticity Directs Stem Cell Lineage Specification. *Cell* 126: 677–689

Fischer T, Hayn A & Mierke CT (2020) Effect of Nuclear Stiffness on Cell Mechanics and Migration of Human Breast Cancer Cells. *Frontiers in Cell and Developmental Biology* 8

Follain G, Herrmann D, Harlepp S, Hyenne V, Osmani N, Warren SC, Timpson P & Goetz JG (2020) Fluids and their mechanics in tumour transit: shaping metastasis.

Fuse N, Hisata K, Katzen AL & Matsuzaki F (2003) Heterotrimeric G Proteins Regulate Daughter Cell Size Asymmetry in Drosophila Neuroblast Divisions C (DaPKC), the G protein subunit Gi, and Partner of Inscuteable (Pins) [1-3]. The depletion of any single api-cal component does not severely affect the cell size. *Current Biology* 13: 947–954

Gallaud E, Pham T & Cabernard C (2017) Drosophila melanogaster neuroblasts: A model for asymmetric stem cell divisions. In *Results and Problems in Cell Differentiation* pp 183–210. Springer Verlag

Han J, Zhang L, Guo H, Wysham WZ, Roque DR, Willson AK, Sheng X, Zhou C & Bae-Jump VL (2015) Glucose promotes cell proliferation, glucose uptake and invasion in endometrial cancer cells via AMPK/mTOR/S6 and MAPK signaling. *Gynecologic Oncology* 138: 668–675

Harding K & White K (2018) Drosophila as a Model for Developmental Biology: Stem Cell-Fate Decisions in the Developing Nervous System.

Harris RE, Pargett M, Sutcliffe C, Umulis D & Ashe HL (2011) Brat Promotes Stem Cell Differentiation via Control of a Bistable Switch that Restricts BMP Signaling. *Developmental Cell* 20: 72–83

Homem CCF & Knoblich JA (2012) Drosophila neuroblasts: A model for stem cell biology. *Development (Cambridge)* 139: 4297–4310

Joe Hirata, Hldeki Nakagosh, Yo-ichi Nabeshima & Fumio Matsuzaki (1988) Asymmetric segregation of the homeodomain protein Prospero during Drosophila development

Kaltschmidt JA, Davidson CM, Brown NH & Brand AH (2000) Rotation and asymmetry of the mitotic spindle direct asymmetric cell division in the developing central nervous system

Karess RE, Chang X-J, Edwards KA, Kulkarni S, Aguilera I & Kiehartt DP (1991) The Regulatory Light Chain of Nonmuscle Myosin Is Encoded by spagheWsquash, a Gene Required for Cytokinesis in Drosophila

Kim KS, Wang H & Zou Q (2009) High speed force-volume mapping using atomic force microscope. In *Proceedings of the American Control Conference* pp 991–996.

Knoblich JA (2010) Asymmetric cell division: Recent developments and their implications for tumour biology. *Nature Reviews Molecular Cell Biology* 11: 849–860 doi:10.1038/nrm3010 [PREPRINT]

Knoblich JA, Jan LY & Nung Jan Y Asymmetric segregation of Numb and Prospero during cell division

Kontomaris & Malamou (2020) Hertz model or Oliver & Pharr analysis? Tutorial regarding AFM nanoindentation experiments on biological samples.

Krieg M, Arboleda-Estudillo Y, Puech PH, Käfer J, Graner F, Müller DJ & Heisenberg CP (2008) Tensile forces govern germ-layer organization in zebrafish. *Nature Cell Biology* 10: 429–436

Lee C-Y, Robinson KJ & Doe CQ (2006a) Lgl, Pins and aPKC regulate neuroblast self-renewal versus differentiation.

Lee CY, Wilkinson BD, Siegrist SE, Wharton RP & Doe CQ (2006b) Brat is a Miranda cargo protein that promotes neuronal differentiation and inhibits neuroblast self-renewal. *Developmental Cell* 10: 441–449

Ludwig T, Kirmse R, Poole K & Schwarz US (2007) Probing cellular microenvironments and tissue remodeling by atomic force microscopy.

Manolaridis I, Kulkarni K, Dodd RB, Ogasawara S, Zhang Z, Bineva G, O'Reilly N, Hanrahan SJ, Thompson AJ, Cronin N, *et al* (2013) Mechanism of farnesylated CAAX protein processing by the intramembrane protease Rce1. *Nature* 504: 301–305

Marques GS, Teles-Reis J, Konstantinides N, Brito PH & Homem CCF (2021) Fate transitions in Drosophila neural lineages: a single cell road map to mature neurons. AUTHORS.

Mauri F, Reichardt I, Mummery-Widmer JL, Yamazaki M & Knoblich JA (2014) The conserved discs-large binding partner banderuola regulates asymmetric cell division in drosophila. *Current Biology* 24: 1811–1825

Mohanty S & Xu L (2010) Experimental Metastasis Assay 1. Sample Preparation 2. Intravenous Injection. *Experimental Metastasis Assay JoVE* 42

Nagelkerke A, Bussink J, Rowan AE & Span PN (2015) The mechanical microenvironment in cancer: How physics affects tumours. *Seminars in Cancer Biology* 35: 62–70

Nava MM, Miroshnikova YA, Biggs LC, Whitefield DB, Metge F, Boucas J, Vihinen H, Jokitalo E, Li X, García Arcos JM, *et al* (2020) Heterochromatin-Driven Nuclear

Softening Protects the Genome against Mechanical Stress-Induced Damage. *Cell* 181: 800-817.e22

Pham TT, Monnard A, Helenius J, Lund E, Lee N, Müller DJ & Cabernard C (2019) Spatiotemporally Controlled Myosin Relocalization and Internal Pressure Generate Sibling Cell Size Asymmetry. *iScience* 13: 9–19

Plodinec M, Loparic M, Monnier CA, Obermann EC, Zanetti-Dallenbach R, Oertle P, Hyotyla JT, Aebi U, Bentires-Alj M, Lim RYH, *et al* (2012) The nanomechanical signature of breast cancer. *Nature Nanotechnology* 7: 757–765

Rachel Kraut, William Chia & Ji.irgen A. Knoblich (1996) Role of inscuteable in orienting asymmetric cell divisions in Drosophila

Radmacher M, Cleveland JP, Fritz M, Hansma HG & Hansma PK (1994) Mapping interaction forces with the atomic force microscope. *Biophysical Journal* 66: 2159–2165

Rebollo E, Roldán M & Gonzalez C (2009) Spindle alignment is achieved without rotation after the first cell cycle in Drosophila embryonic neuroblasts. *Development* 136: 3393–3397

Reiter LT, Potocki L, Chien S, Gribskov M & Bier E (2001) A Systematic Analysis of Human Disease-Associated Gene Sequences In Drosophila melanogaster.

Rorth P (1996) A modular misexpression screen in Drosophila detecting tissue-specific phenotypes. *Genetics* 93: 12418–12422

Roubinet C & Cabernard C (2014) Control of asymmetric cell division. *Current Opinion in Cell Biology* 31: 84–91 doi:10.1016/j.ceb.2014.09.005 [PREPRINT]

Sanes DH, Reh TA & Harris WA (2012) Determination and differentiation. *Development of the Nervous System*: 77–104

Sarwar M, Sykes PH, Chitcholtan K & Evans JJ (2020) Extracellular biophysical environment: Guilty of being a modulator of drug sensitivity in ovarian cancer cells. *Biochemical and Biophysical Research Communications* 527: 180–186

Schaefer M, Shevchenko A, Shevchenko A & Knoblich JA (2000) A protein complex containing Inscuteable and the Gα α-binding protein Pins orients asymmetric cell divisions in Drosophila

Schneider I (1964) Differentiation of Larval Drosophila Eye-antenna1 Discs in Vitro ’

Schwartz BL, Yin Z, Magin RL, Sinkus R, Lorenzen J, Schrader D, Lorenzen M, Dargatz M & Holz D (2000) Physics in Medicine & Biology To cite this article: R Sinkus et al

Sinha Ray S (2013) Structure and Morphology Characterization Techniques. *Clay-Containing Polymer Nanocomposites*: 39–66

Sonoda J & Wharton RP (2001) Drosophila brain tumor is a translational repressor. *Genes and Development* 15: 762–773

Suresh S (2007) Biomechanics and biophysics of cancer cells. *Acta Biomaterialia* 3: 413–438

Suzuki H & Mashiko S (1998) Adhesive force mapping of friction-transferred PTFE film surface

Tolwinski Nicholas (2017) Introduction:Drosophila—A Model System forDevelopmental Biology.

Touhami A, Nysten B & Dufrêne YF (2003) Nanoscale Mapping of the Elasticity of Microbial Cells by Atomic Force Microscopy.

Weng R & Cohen SM (2015) Control of Drosophila Type I and Type II central brain neuroblast proliferation by bantam microRNA.

Wenger MPE, Bozec L, Horton MA & Mesquidaz P (2007) Mechanical properties of collagen fibrils. *Biophysical Journal* 93: 1255–1263

Woodhouse EC & Chuaqui RF (1997) Skeletal Complications of Malignancy mors-including breast, prostate, and lung-frequently metastasize American Cancer Society

Wullkopf L, West AK v., Leijnse N, Cox TR, Madsen CD, Oddershede LB & Erler JT (2018) Cancer cells' ability to mechanically adjust to extracellular matrix stiffness correlates with their invasive potential. *Molecular Biology of the Cell* 29: 2378–2385

Yadav S, Barton MJ & Nguyen NT (2019) Biophysical properties of cells for cancer diagnosis. *Journal of Biomechanics* 86: 1–7 doi:10.1016/j.jbiomech.2019.02.006 [PREPRINT]

Young W, Tanner SK & Tanner K (2021) Emerging principles of cancer biophysics Peer Review.

Yu F, Morin X, Cai Y, Yang X & Chia W (2000) Analysis ofpartner of inscuteable, a Novel Player of Drosophila Asymmetric Divisions, Reveals Two Distinct Steps in Inscuteable Apical Localization

Yuan HX, Xiong Y & Guan KL (2013) Nutrient Sensing, Metabolism, and Cell Growth Control. *Molecular Cell* 49: 379–387 doi:10.1016/j.molcel.2013.01.019 [PREPRINT]

Zhang Y, Rai M, Wang C, Gonzalez C & Wang H (2016) Prefoldin and Pins synergistically regulate asymmetric division and suppress dedifferentiation OPEN.